

Title of the project:

Chemical tuning of organometal halide perovskites for solar cell applications

Starting date and duration:

1 September 2014, PhD position for four years

Applicant:

M.E. Kamminga

Promotor:

Prof. Dr. T.T.M. Palstra

Abstract:

Organometal halide perovskites have recently obtained high power-to-electrical conversion efficiencies of over 15% in simplified planar heterojunction solar cell devices. No nanostructuring was optimized to achieve these high efficiencies. This breakthrough makes organometal halide perovskites as absorber material promising for highly efficient and easily processable solar cells. Organometal halide structures are hybrid structures that contain inorganic metal halides and organic ligands that both can be tuned. Changing the chemical composition of these hybrid materials will change its structural parameters, such as distances and angles that define the perovskite structure. These chemical changes and the way in which the absorber layer is deposited will influence its physical properties; electron/hole mobility, dielectric constant, size of the band gap, exciton diffusion length, exciton binding energy and exciton lifetime. As a result, this will influence the solar cell device performance. In this proposal, the goal is to obtain insight into the materials properties in relation to the device performance. Knowledge of the working principle of these devices will make it possible to investigate ways to chemically tune its physical properties and hence its performance. As a result, improvement of the existing concept of solar cells based on perovskite absorber layers will be expected.

Introduction

Solar cells are part of the strategy towards carbon-neutral energy sources [1] [2]. Inorganic silicon solar cells have been reported with power conversion efficiencies up to 25% [3]. However, these devices have certain limitations, such as heavy weight and high fabrication cost. To overcome these limitations, the search for alternative solar cells has increased tremendously. This has resulted in the development of organic and various thin-film solar cells [4]. However, efficiencies comparable to the silicon solar cell have yet to be achieved.

The dye-sensitized solar cell (DSC), invented in 1991 by O'Regan and Grätzel, is an easily processable, stable and low-cost solar cell that has a reasonably high efficiency of 12% [5]. DSCs are hybrid solar cells that contain an *inorganic* n-type oxide (such as TiO_2) with an organic or metal complex dye as sensitizer, infiltrated in an *organic* p-type hole-conductor [5]. DSCs are an attractive alternative to the existing solid-state p-n junction solar cells. Efficiencies of over 12% have been achieved using a liquid electrolyte [6]. Fully solid-state DSCs are less efficient than liquid DSCs, mainly because of the rapid carrier recombination that is possible at the device interfaces [7]. However, the use of liquid DSCs is disadvantageous for industrial applications. There is a variety of sensitizers that can be used in DSCs and it can be advantageous to implement inorganic semiconductors in the form of quantum dots as sensitizer, because semiconductor quantum dots possess a large intrinsic dipole moment. Moreover, their band gap can be tuned by controlling their size and shape, and this tunability is a useful property in light-absorber materials [8]. In 2013, a solid-state DSC with an efficiency of 12% under AM1.5 illumination (100 mW/cm^2) was published, using an organometal trihalide perovskite absorber with the general formula $(\text{RNH}_3)\text{BX}_3$ (where R is $\text{C}_n\text{H}_{2n+1}$, X is the halogen I, Br or Cl, and B is Pb or Sn [9]) instead of the dye [10]. This solid-state DSC has obtained an efficiency similar to the liquid-type DSC. Therefore, organometal halide perovskites turn out to be promising materials for high-efficiency nanostructured devices [10].

Recent studies, however, showed that nanostructuring is not necessary to achieve high solar-to-electrical power conversion efficiencies [11]. Designing a relatively simple planar heterojunction solar cell with a vapour-deposited perovskite absorber layer has resulted into efficiencies of over 15%. This is a serious breakthrough in the field of solar cell research, as the focus has been primarily on organic and conventional DCS solar cells so far. Organometal halide perovskites as absorber materials in solar cell devices are promising for creating both highly efficient and easily processable solar cells. This makes it a serious competitor to the silicon solar cell. Since this is a completely new line of research, the physics behind the operating principles is hardly known and improvements are certain. This research proposal will focus on revealing the physical principles that govern the high efficiencies generated by organometal halide perovskites as absorber layer in solar cells. To begin with, an overview of the research in this area is given. Subsequently, the main goals and research questions of this proposed research are stated. Finally, the proposed research methods are described.

Perovskite absorber layers in solar cells

Organic-inorganic hybrid frameworks are crystalline materials in which organic and inorganic structural elements co-exist on the molecular scale within a single phase. The structure of hybrids is based on Metal-Organic Frameworks (MOFs) and perovskites. MOFs contain coordination bonds between metal cations and electron donors, such as amine groups. This results in the formation of three-dimensional clusters. MOFs are porous structures and applicable in gas storage, gas separation, gas purification, catalysis and sensors [12].

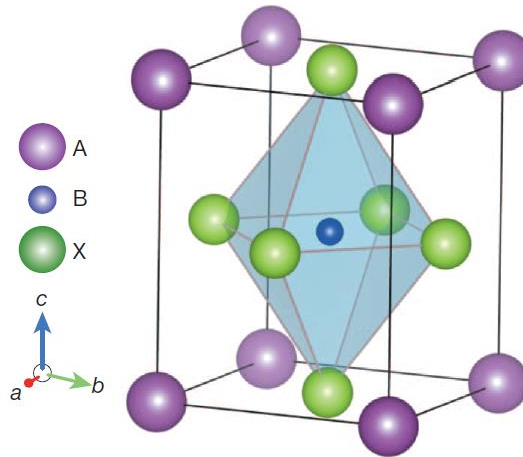


Figure 1: Schematic representation of perovskite structure in the ABX₃ form. A represents the methylammonium, B the Pb and X is I or Cl. Figure adapted from [11].

Perovskite structures contain corner-sharing [BX₆] octahedra. A schematic representation of the perovskite structure is shown in figure 1. Perovskites are building blocks for many physical properties such as superconductivity and magnetoresistance [13]. The combination of MOFs and perovskites results in the layered organic-inorganic compounds called *hybrids*. Hybrids contain organic perovskite sheets with corner-sharing octahedra and organic spacers, as can be seen in figure 2. Due to the combination of organic and inorganic elements, hybrid structures contain various interesting properties in the field of condensed matter physics: magnetism and optical, electrical and dielectrical properties [14]. These materials received increasing interest for various applications, such as for combining its solubility with ferromagnetism and semiconductivity to be applicable in soluble electronics [15].

Kojima *et al.* pioneered in implementing organic-inorganic structures into solar cells [16]. They used organic-inorganic lead halide perovskite compounds (CH₃NH₃)PbBr₃ and (CH₃NH₃)PbI₃ as visible-light sensitizers in photoelectrochemical cells. The reasons for implementing organic-inorganic perovskites in cells are that - besides having unique optical properties [17], excitonic properties [18] and electrical conductivity [19] - these hybrid materials are easily synthesized using abundant sources: Pb, C, N and halogens. X-ray diffraction analysis of spin-coated (CH₃NH₃)PbBr₃ and (CH₃NH₃)PbI₃ in precursor solutions on

TiO₂ showed that both materials exhibit crystalline nanostructures in the perovskite ABX₃ form [16], as shown in figure 1.

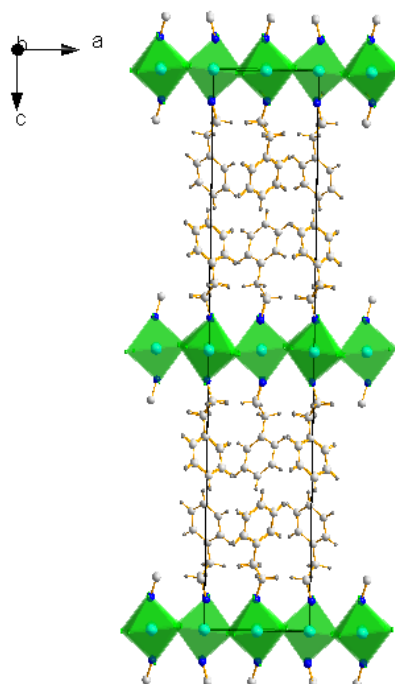


Figure 2: Layered organic-inorganic hybrid structure. Figure adapted from analysis of single-crystal X-ray diffraction data measured and presented (Nanosymposium 26 June 2013) by M.E. Kamminga.

Depositing lead halide perovskite nanocrystals on mesoporous TiO₂, with quantum dot sizes of 2-3 nm, achieved an energy conversion efficiency of 3.8% in a photoelectrochemical cell [16]. Even higher values of 6.54% were obtained with liquid junction cells based on quantum dot sensitized TiO₂ films and an iodide/triiodide based redox electrolyte [20]. However, the (CH₃NH₃)PbI₃ perovskite nanoparticles are unstable in the iodide-containing liquid electrolyte due to rapid dissolution of the perovskite in the electrolyte. Kim *et al.* showed that this stability improves remarkably when a solid-state device is used [21]. Figure 3 shows the device performance over a time range of 500 hours when the solar cells were stored in air, at room temperature, without encapsulation.

This solid-state mesoscopic solar cell employing (CH₃NH₃)PbI₃ perovskite nanocrystals as a light absorber and spiro-OMeTAD as a hole transporting layer obtained a high stability. Moreover, an efficiency of 9.7% under AM 1.5 illumination was reached [21]. An even higher efficiency of over 12% was obtained when PTAA was used as hole transporting layer, instead of spiro-OMeTAD [10]. This is because the small molecular spiro-OMeTAD can more easily infiltrate in the mesoporous-TiO₂ layer than the high-molecular-weight polymer PTAA. Therefore, extracting charge carriers becomes more effective when using PTAA. The short diffusion length of excitons to the TiO₂/(CH₃NH₃)PbI₃ interface requires no unnecessary displacement over long distances [10].

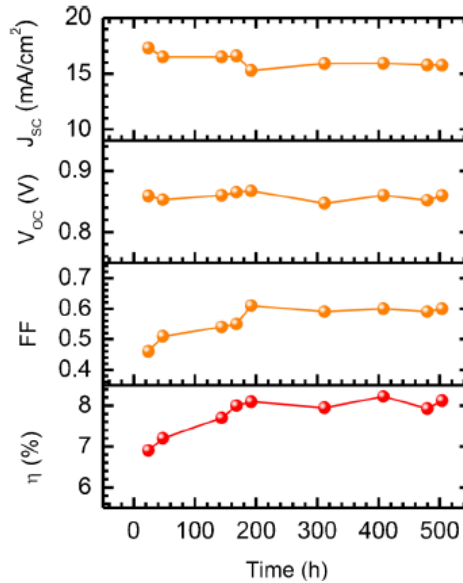


Figure 3: Device performance of a $(\text{CH}_3\text{NH}_3)\text{PbI}_3$ sensitized solid-state solar cell stored in air, at room temperature, without encapsulation. A high stability is shown. Measurements were performed under one sun illumination. Figure adapted from [21].

A recent breakthrough in this field is that nanostructuring is not necessary in order to achieve high efficiencies with organometal halide perovskite materials [11]. A simple planar heterojunction solar cell with vapour-deposited perovskite as absorbing layer can reach efficiencies of over 15%. This results in highly efficient and simplified solar cell devices that do not need complex nanostructures. This is highly promising for future applications. Mixed halide perovskites $(\text{CH}_3\text{NH}_3)\text{PbI}_{3-x}\text{Cl}_x$ are found to operate relatively efficiently as a thin-film absorbers in solution-processed planar heterojunction solar cells with no mesostructure involved [22]. This is the first example of a perovskite-based solar cell that can operate in conventional thin-film architecture where the perovskite absorber layer performs charge-separation and charge-transport of both carriers. Moreover, Docampo *et al.* demonstrated that a planar heterojunction solar cell can deliver a power-conversion efficiency up to 6.5% when an indium-doped tin oxide (ITO)-coated plastic foil is used as substrate [23]. Figure 4 shows this flexible perovskite solar cell. This makes various future applications possible.

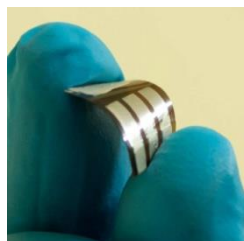


Figure 4: Picture of the first flexible perovskite solar cell. Figure adapted from [23].

Liu *et al.* investigated the difference between device performances of this conventional type of solar cell with vapour-deposited and solution-processed perovskite absorber layers [11]. Figure 5 illustrates the dual-source vapour-deposition setup and the device structure of this solar cell. From the bottom up (light is incident from the bottom), a

compact layer of n-type TiO_2 is constructed on a fluorine-doped tin oxide (FTO)-coated glass substrate. This acts as the electron selective contact. Subsequently, the perovskite layer is deposited on the n-type layer, and followed by spiro-OMeTAD. Spiro-OMeTAD is the p-type hole conductor, which brings the holes to the silver cathode. The perovskite absorber is solution-processed or vapour-deposited, while the n-type compact layer and p-type hole transporter are solution-processed in both cases.

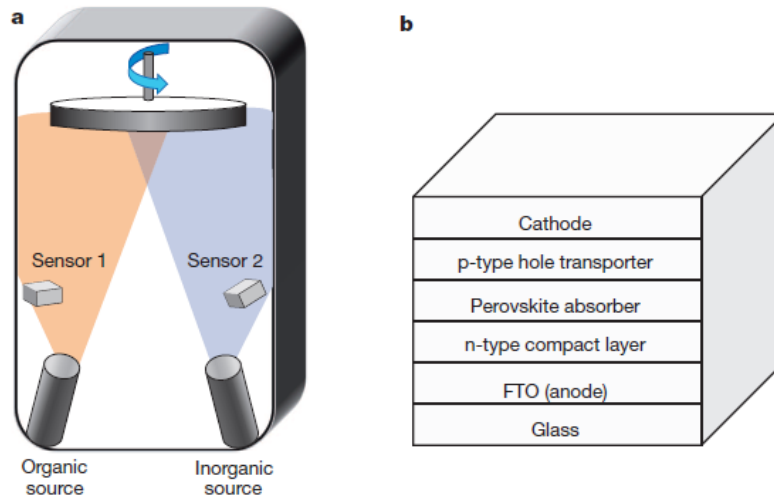


Figure 5: a. Dual-source thermal evaporation system used for depositing a flat film of mixed halide perovskite absorber layer; the organic source contained methylammonium iodide and the inorganic source contained PbCl_2 . b. Device structure of planar heterojunction p-i-n perovskite solar cell. Figures adapted from [11].

Comparison of solar cell devices with either vapour-deposited or solution-processed perovskite absorber layer was done by X-ray diffraction, scanning electron microscopy and based on device performances. The results are summarized below.

X-ray diffraction (XRD). As can be seen in figure 6, the main diffraction peaks are in identical positions for both techniques, which means that they gave the same mixed-halide perovskite with an orthorhombic crystal structure [24].

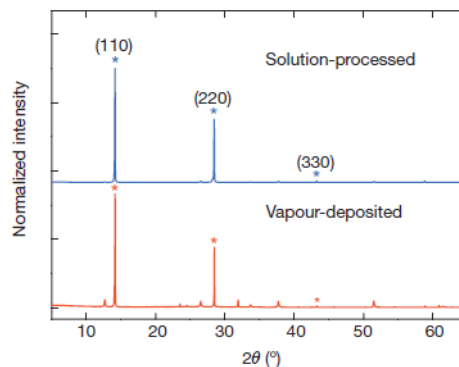


Figure 6: X-ray diffraction spectra of solution-processed and vapour-deposited perovskite films. The intensities are normalized. Figure adapted from [11].

Scanning electron microscopy (SEM). Figure 7 shows various scanning electron microscopy (SEM) images of the films made by solution-processing and vapour-deposition. From the top view - images a and b - it is clear that vapour-deposited perovskite films are extremely uniform, while solution-processed films are not. They show crystalline ‘platelets’ on a length scale of tens of micrometers. Moreover, the voids between these ‘platelets’ appear to extend directly to the TiO₂. The cross-sectional images c and d show again that the vapour-deposited perovskite layer is uniform, while the solution-processed perovskite film is extremely smooth, with very large grain sizes. Zooming out, as in images e and f, makes it clear that the vapour-deposited film is flat, with an average thickness of approximately 330 nm, while the solution-processed film has a thickness varying from 50 to 465 nm. Note that this image is a cross-section of a single ‘platelet’ as indicated in image b, meaning that the overall thickness variation is even bigger; ranging from 0 to 465 nm.

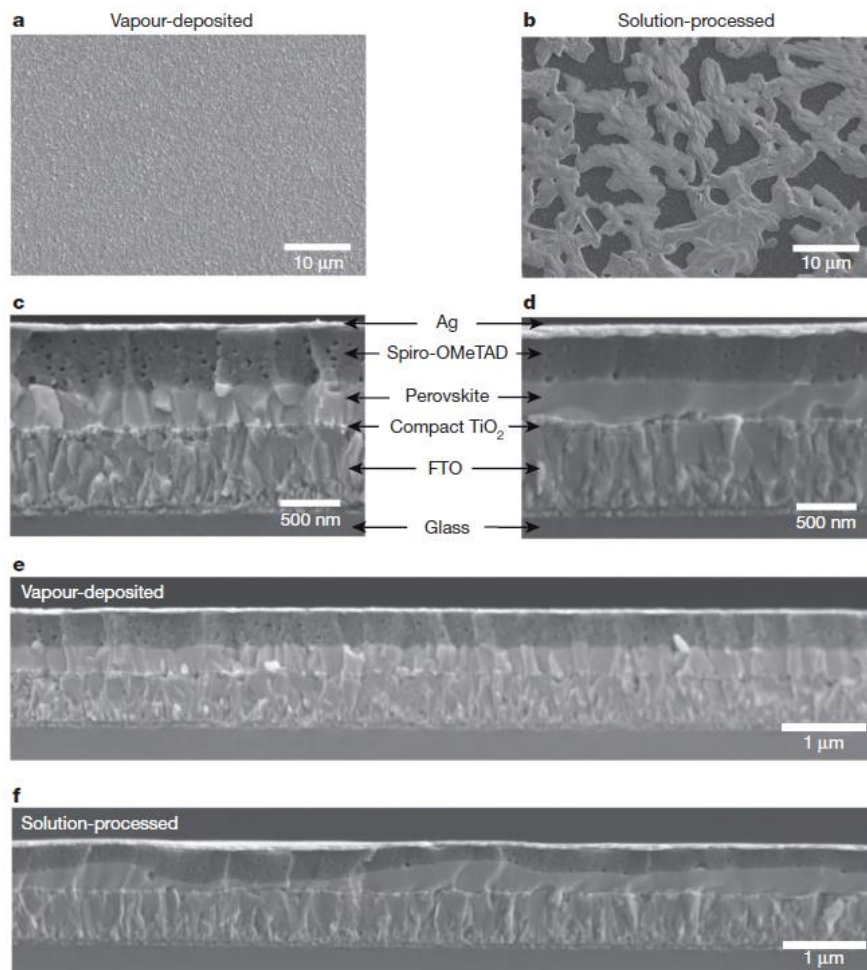


Figure 7: SEM images from vapour-deposited and solution-processed perovskite films. a and b are top views and c-f are cross-sections of the device. Figures adapted from [11].

Device performance. The vapour-deposited and solution-processed perovskite solar cells obtained different device performances. The vapour-deposited solar cell obtained an efficiency of over 15%, while the solution-processed solar cell obtained an efficiency of 8.6%. The reason for this difference in device performances can be found in the film thickness. The

thickness needs to be optimized with respect to the exciton diffusion length. When the film is too thin, it will not absorb enough sun light; when the film is thicker than the exciton diffusion length, the charge will not be collected at the n-type and p-type heterojunctions. Stranks *et al.* [25] reported that the exciton diffusion lengths are greater than one micrometer in the mixed-halide $(\text{CH}_3\text{NH}_3)\text{PbI}_{3-x}\text{Cl}_x$ perovskite and around 100 nanometers in the $(\text{CH}_3\text{NH}_3)\text{PbI}_3$ perovskite. However, it is still unclear why the small addition of chloride ions results in such an increase in the electron-hole diffusion length.

In the work of Lui *et al.*, the solution-processed perovskite layer resulted in lower device performance compared to the vapour-deposited perovskite layer [11]. The thickness variation in the solution-processed layer is enormous, as can be seen in figure 7b. There are voids in the layer that extend directly to the TiO_2 , providing a direct contact between the p-type spiro-OMeTAD and the n-type TiO_2 . This creates shunting paths, which are probably partially responsible for the lower fill factor and open-circuit voltages of the solution-processed planar heterojunction device. However, it is still remarkable that the solution-processed devices perform with efficiencies over 8%.

The work of Lui *et al.* is based on an engineering approach [11]. Despite the high efficiencies that were obtained, no insight in the physical principles behind the results is given. The question remains how the primary excitation works, what the nature of the excited state is and what the mechanisms for free-charge generation in these organometal halide perovskite materials are.

Main goals and research questions

The two central questions of this research proposal are:

1. *How can the physical properties of the organometal halide perovskite absorber layer be changed chemically?*
2. *How does the physical properties of the organometal halide perovskite absorber layer relate to the solar cell device performance?*

The motivation for these research questions is that perovskite solar cells have turned out to be serious competitors to silicon solar cells, because of their high performance and easy processability [11]. However, besides the fact that this is a relatively easy way to make highly efficient solar cells, it is a particularly new line of research and the physics behind the operating principles is hardly known. Improvements are certain. Therefore, it is useful to understand the working principle of these devices in order to investigate ways to tune its physical properties and hence its performance. As a result, improvement of the existing concept of solar cells based on perovskite absorber layers will be expected. Thus far, Lui *et al* [11] tried to improve the performance by adjusting the solar cell by changing the TiO₂ layer and changing the deposition technique. However, investigating the intrinsic properties of the perovskite absorber layer itself by changing its chemistry has yet to be done. This research proposal will focus on revealing the physical principles that govern the high efficiencies generated by organometal halide perovskites as absorber layer in solar cells.

The proposed research project contains the following three main goals:

1. To change the physical properties of the perovskite absorber layer by changing its chemical composition and morphology;
2. To relate the chemical composition of the perovskite absorber layer to its physical properties: electron/hole mobility, dielectric constant, size of the band gap, exciton diffusion length, exciton binding energy and exciton lifetime;
3. To relate the physical properties of the perovskite absorber layer to the solar cell device performance: open-circuit voltage, short-circuit current, fill factor, power conversion efficiency and external quantum efficiency.

In all previous work, Pb²⁺ was used as the metal in the organometal halides. Reason for this is probably that Ge²⁺, Pb²⁺ and Sn²⁺ have the best optoelectronic properties and therefore the highest potential in device applications [9]. Thus far, only Pb²⁺ has been reported in the literature, but lead is toxic and it is noteworthy to look for alternatives such as Sn²⁺. Furthermore, Lui *et al.* obtained better device performances when using mixed-halide perovskites with a mixture of iodide and chloride [11]. Stranks *et al.* reported that addition of a small amount of chloride in (CH₃NH₃)PbI₃ resulted into an enormous increase in exciton diffusion length, which could encounter for the better device performance [25]. However, the reason for this is still unknown. From the moment Kojima *et al.* pioneered with implementing CH₃NH₃ as ligand in the perovskite [16], this has been the only ligand reported

for solar cell applications yet. The properties of perovskite materials are strongly dependent on the ligands [15]. Replacing these ligands, for example with longer or aromatic ligands, will influence the physical properties of the films and therefore the device performance. Figure 8 shows various examples of ligands that can be used.

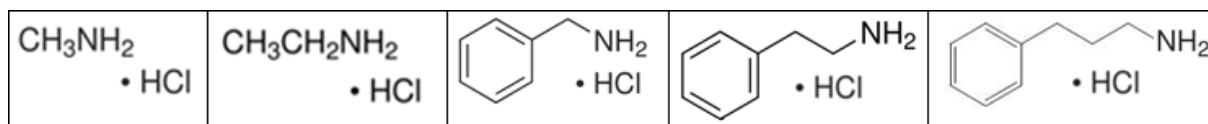


Figure 8: Examples of ligands that can be used. From left to right: methylamine hydrochloride, ethylamine hydrochloride, benzylamine hydrochloride, 2-phenylethylamine hydrochloride, 3-phenyl-1-propylamine hydrochloride. Figures adapted from www.sigmaaldrich.com.

The main goal here is to find a relationship between the structural parameters of various hybrid films and physical properties of the thin films. The structural parameters include distances and angles within the perovskite structure and, in particular, the binding of the amine groups of the ligands to the metal halide octahedra, as investigated by Polyakov *et al.* [26] for analogous hybrids. The physical properties include the electron/hole mobility, dielectric constant, size of the band gap, exciton diffusion length, exciton binding energy and exciton lifetime. The operating principle of a solar cell contains the following five steps: absorption of light and generation of excitons, exciton migration, exciton dissociation (i.e. charge separation), charge transport and charge collection. The band gap of the absorber layer determines what portion of the solar spectrum will be absorbed by the solar cell. Tuning this band gap will influence the device performance. The dielectric constant should be determined, because it is the driving force for electron hole splitting and hence the formation of an exciton, which is the key component in solar cell device operation. The excitons formed due to light absorption should lead to the formation of free charge carriers. Determination of the exciton binding energy is important to find the barrier to overcome in order to separate the electron from the hole. The average distance an exciton can diffuse through a material before annihilation by recombination is the exciton diffusion length. For this, the exciton lifetime is an important factor. Knowledge of the exciton diffusion length is important for determining the optimal thickness of the absorber layer in order to minimize the losses through recombination of charge carriers. Determination of electron/hole mobility is of importance, because charge transport is a key phenomenon in solar cell operation. This mobility accounts for charge collection and losses through recombination.

Optimization of the solar cell device performance includes three main steps. The first step is to investigate what the ultimate thickness of the perovskite layer is, for which the exciton diffusion length should be determined precisely. This is strongly dependent on the type of material and the crystallinity and therefore the deposition technique. The second step is to investigate the tunability of the band gap of the perovskite layer, by making mixed hybrids; mixed halide, mixed metal and mixed ligand hybrids. The amount of doping in this way will change the band gap. The third step is to give an explanation on how the deposition technique and therefore the surface chemistry will influence the device performance.

Approach and methods

This section summarizes the approaches and methods that will be followed during the proposed research project. The next section will give a timeline.

Synthesis of hybrid materials. The synthesis procedure that will be used is the one investigated by Arkenbout [15]. The organic and inorganic components will be combined in solution, after which the hybrids crystallize by self-assembly. The inorganic components consist of divalent transition metal halides and the organic components are conjugated amines containing various chemical groups, such as alkane, benzene, anthracene, thiophene or fluorine groups (see figure 8 for various examples). The organic compounds, for example methylammonium chloride, are made by slowly adding a saturated aqueous hydrogen chloride solution to methylamine. The crystalline compound created can then be washed with water, dried in air and stored as powder. The general procedure that will be followed to form the hybrids is to mix the organic compound with the inorganic compound in a ratio of 2:1 in ethanol and water and to heat it in a water bath to 50 °C until it has solved. The solutions will be stored for a couple of days in the oven at 60 °C to crystallize.

Creating well-defined surfaces. In order to determine the physical parameters precisely, it is important to create well-defined surfaces. Therefore, the perovskite absorber layers will be formed from single crystals and from Langmuir-Blodgett deposition. X-ray photoelectron spectroscopy (XPS) will be used to analyse the surface chemistry. SEM images will show the thickness variation and the homogeneity of the layers.

Investigating structural properties. The characterization of the synthesized hybrids will be carried out by performing XRD experiments with the Bruker d8 powder diffractometer and the Bruker Apex single crystal diffractometer in order to obtain structural parameters such as bond lengths and angles between the atoms.

Investigating electrical properties. The solar cell devices will be build up from the components illustrated in figure 5b. The current-voltage characteristics will be measured in dark and under irradiation from an AM1.5 solar light simulator. From this, the open-circuit voltage, short-circuit current, fill factor and power conversion efficiency will be adapted. The dielectric constants will be measured with the aid of a Quantum Design Physical Properties Measurement System (PPMS). This measurement will be performed by placing the perovskite structure between two metal contacts and making it into a parallel plate capacitor with the perovskite as medium in between. The carrier mobility will be measured by making a field effect transistor out of the perovskite layers by planting a gate on top.

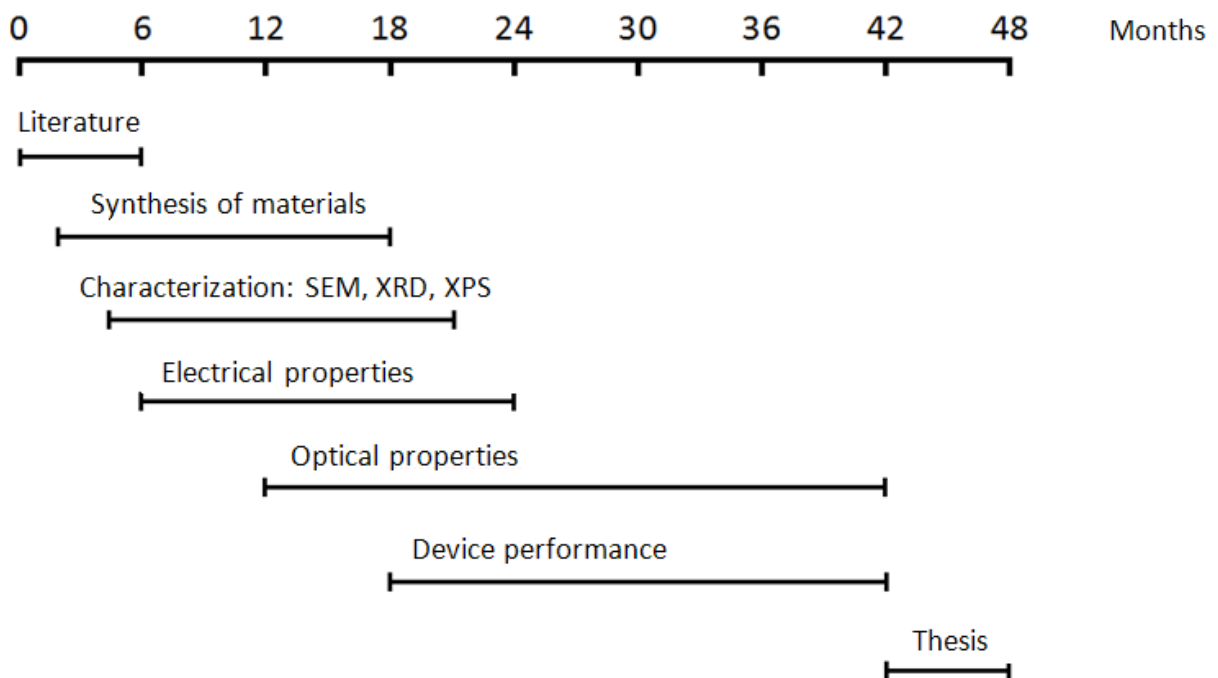
Investigating optical properties. The optical properties of the solar cell devices will be investigated in collaboration with the Photophysics and OptoElectronics group of Prof. Dr. M.A. Loi. The measurements include steady-state photoluminescence (PL) and time-resolved photoluminescence (TRPL) measurements. The band gap of the absorber layer will be determined from the absorption spectra. In these spectra, the exciton binding energies will be visible in the form of small absorption peaks. Investigation of the difference between the absorption and emission spectra will give insight into the energy distribution over the

molecules in the system. The exciton diffusion length will be determined from the diffusion coefficients from the model reported by Stranks *et al.* [25]. TRPL measurements show the decay of photoluminescence with respect to time. The decay time, i.e. the lifetime of excitons before recombination takes place, can be adapted from these spectra.

Once all data will be obtained, it is proposed to look for a relation or trend between the various variables.

Project timeline

The following timeline gives an overview of the work that will be done in the 48 months of the project.



Cost estimates

Personnel positions

One PhD position for four years.

Budget: k€ 204 for total of four years

Running budget

Standard expenses for one experimental position; including conference participation and maintenance of equipment.

Budget: k€ 15 per year. k€ 60 for total of four years.

Equipment

Available equipment:

- Chemistry lab with fume hoods and other chemical tools
- Glove box
- Bruker d8 powder diffractometer
- Bruker Apex single crystal diffractometer
- Quantum Design Physical Properties Measurement System (PPMS)

Required equipment:

- Characterization of photophysical properties in collaboration with Loi-group.
- SEM with De Hosson-group
- Making Langmuir-Blodgett films with Rudolf-group.
- Device modelling with J.A. Koster.

Other support

Other support will be given by the senior scientist and technician via the Zernike Institute for Advanced Materials and the University of Groningen.

Budget summary

A summary of the expenses is given in the following table. All amounts are given in k€.

	2014	2015	2016	2017	2018	TOTAL
Personnel (positions):						
PhD students	1/3	1	1	1	2/3	4
Postdocs	-	-	-	-	-	-
Technicians	-	-	-	-	-	-
Guests	-	-	-	-	-	-
Personnel (costs)	17	51	51	51	34	204
Running budget	5	15	15	15	10	60
Equipment	-	-	-	-	-	-
TOTAL requested	22	66	66	66	44	264

References

- [1] F.C. Chen, C.J. Ko, J.L. Wu & W.C. Chen, *Sol. Energ. Mat. Sol. C.*, 2010, **94**, 2426-2430
- [2] G. Yu, J. Gao, J.C. Hummelen, F. Wudl & A.J. Heeger, *Science*, 1995, **270**, 1789-1791.
- [3] M.A. Green, K. Emery, Y. Hishikawa, W. Warta & E.D. Dunlop, *Prog. Photovoltaics*, 2012, **20**, 606-614.
- [4] K.L. Chopra, P.D. Paulson & V. Dutta, *Prog. Photovolt: Res. Appl.*, 2004, **12**, 69-92.
- [5] B. O'Regan & M. Grätzel, *Nature*, 1991, **353**, 737-740.
- [6] A. Yella, H.-W. Lee, H.N. Tsao, C. Yi, A.K. Chandiran, Md.K. Nazeeruddin, E.W.-D. Diau, C.-Y. Yeh, S.M. Zakeeruddin & M. Grätzel, *Science*, 2011, **334**, 629-634.
- [7] P.P. Boix, Y.H. Lee, F. Fabregat-Santiago, S.H. Im, I. Mora-Sero, J. Bisquert & S.I. Seok, *ACS Nano*, 2012, **6**, 873-880.
- [8] P.V. Kamat, *J. Phys. Chem. C*, 2008, **112**, 18737-18753.
- [9] Z. Cheng & J. Lin, *CrystEngComm*, 2010, **12**, 2646-2662.
- [10] J.H. Heo, S.H. Im, J.H. Noh, T.N. Mandal, C.-S. Lim, J.A. Chang, Y.H. Lee, H. Kim, A. Sarkar, Md.K. Nazeeruddin, M. Grätzel & S.I. Seok, *Nature Photon.*, 2013, **7**, 486-491.
- [11] M. Lui, M.B. Johnston & H.J. Snaith, *Nature*, 2013, **501**, 395-398.
- [12] J. Čejka, *Angew. Chem. Int. Ed.*, 2012, **51**, 4782-4783.
- [13] B. Raveau, *Prog. Solid State Chem.*, 2007, **35**, 171-173.
- [14] C.N.R. Rao, A.K. Cheetham & A. Thirumurugan, *J. Phys. Condens. Matter*, 2008, **20**, 083202.
- [15] A.H. Arkenbout, *PhD thesis series*, Zernike Institute, 2010.
- [16] A. Kojima, K. Teshima, Y. Shirai & T. Miyasaka, *J. Am. Chem. Soc.*, 2009, **131**, 6050-6051.
- [17] N. Kitazawa, Y. Watanabe & Y. Nakamura, *J. Mater. Sci.*, 2002, **37**, 3585-3587.
- [18] K. Tanaka, T. Takahashi, T. Ban, T. Kondo, K. Uchida & N. Miura, *Solid State Commun.*, 2003, **127**, 619-623.
- [19] K. Yamada, H. Kawaguchi, T. Matsui, T. Okuda & S. Ichiba, *Bull. Chem. Soc. Jpn.*, 1990, **63**, 2521-2525.

- [20] J.-H. Im, C.-R. Lee, J.-W. Lee, S.-W. Park & N.-G. Park, *Nanoscale*, 2011, **3**, 4088-4093.
- [21] H.-S. Kim, C.-R. Lee, J.-H. Im, K.-B. Lee, T. Moehl, A. Marchioro, S.-J. Moon, R. Humphrey-Baker, J.-H. Yum, J.E. Moser, M. Grätzel & N.-G. Park, *Sci. Rep.*, 2012, **2**, 0591.
- [22] J.M. Ball, M.M. Lee, A. Hey & H.J. Snaith, *Energy Environ. Sci.*, 2013, **6**, 1739-1743.
- [23] P. Docampo, J.M. Ball, M. Darwich, G.E. Eperon & H.J. Snaith, *Nat. Commun.*, 2013, **4**, 2761.
- [24] M.M. Lee, J. Teuscher, T. Miyasaka, T.N. Murakami & H.J. Snaith, *Science*, 2012, **338**, 643-647.
- [25] S.D. Stranks, G.E. Eperon, G. Grancini, C. Menelaou, M.J.P. Alcocer, T. Leijtens, L.M. Herz, A. Petrozza & H.J. Snaith, *Science*, 2013, **342**, 341-344.
- [26] A.O. Polyakov, A.H. Arkenbout, J. Baas, G.R. Blake, A. Meetsma, A. Caretta, P.H.M. van Loosdrecht & T.T.M. Palstra, *Chem. Mater.*, 2012, **24**, 133-139.

Curriculum Vitae – Machteld Kamminga

Personal

Name: Machteld Elizabeth Kamminga
Place of birth: Wageningen
Date of birth: 15 September 1991
Nationality: Dutch
Address: Parkweg 79A
City: 9725 ED Groningen
Phone number: 06-30184146
Email: m.e.kamminga@gmail.com

Education

09/2012 – M.Sc. Nanoscience, Topmaster Programme.
08/2014: Faculty of Mathematics and Natural Sciences, University of Groningen. The Netherlands.
Small project: Revealing the influence of the organic part of Cu-based hybrids on its properties.
Grade: 9.
Thesis: Development of new flow cell device for single-molecule DNA replication studies. (Expected 31-08-2014)

02/2010 – Honours College, extracurricular Bachelor programme, designed
08/2012: for top students to broaden their knowledge within and between the faculties of the University of Groningen. The Netherlands.
Courses and projects in debating, academic writing, medicine, history of arts, nuclear energy and isotope research.

09/2009 – B.Sc. Applied Physics.
08/2012: Faculty of Mathematics and Natural Sciences, University of Groningen. The Netherlands.
Propaedeutics Cum Laude.
Thesis: Scanning Probe Microscopy applied to GaSb and GeSb thin films.
Grade: 8.

Work experience

10/2011 – Member of *Promoteam Natuurkunde*, University of Groningen.
02/2013: Promoter of (applied) physics Bachelor and Masters, including organizing various events such as ‘Student for a Day’ to give people a feel of studying physics.

- 08/2011 – Physics and astronomy member *Bètasteunpunt*, University of
02/2013: Groningen. Online e-mail help desk for high school students who need help with their physics and/or astronomy projects and papers.
- 09/2011 – Mentor of twelve first-year (applied) physics students. University
08/2012: of Groningen.
- 11/2011 – Teaching assistant, undergraduate course in Thermodynamics.
02/2012: University of Groningen.
- 09/2011 – Lab assistant, undergraduate course in first-year physics.
11/2011: University of Groningen.
- 2007 – Tutoring and exam training for various high school students; in physics,
2011: chemistry and mathematics.

Other activities

- 10/2013 – BAC Tenure-Track Clinical Applications of Bio- and Nanomaterials,
present: student member.
- 10/2012 – Member of the Course Committee Nanoscience.
present:
- 09/2010 – ‘Role model’ on www.spiegelbeeld.net; *VHTO, Landelijk expertisebureau*
present: *meisjes/vrouwen en bèta/techniek*. Visiting high schools to inform girls about studying natural sciences.

Certificates and computer skills

Laser Safety Certificate (expected 06-02-2014).
BLS/CPR certified, Nederlandse Hartstichting.
Computer skills: MS Office, OriginLab, LabVIEW, ImageJ, Gwyddion, Diamond 3, NT-MDT.

Languages

Dutch: mother tongue
English: fluent
German: moderate
French: basic
Spanish: basic



Declaration of hospitality and financial support for research costs

Appendix to the Proposal for a PhD research position
in the NWO Graduate Programme Advanced Materials, deadline 2 Feb. 2014

Name of the applicant: Machteld Elizabeth Kamminga

Title of the proposal: Chemical tuning of organometal halide perovskites for solar cell applications

By signing this document the staff member declares that she/he is willing to host and supervise the PhD research project that is mentioned above. In addition, the staff member declares that she/he has and makes available the materials, infrastructure and the funding that is needed for covering the research costs (the costs in addition to the salary of the PhD student some funding for travel and training), as described in the proposal.

The signing staff members must be affiliated with the Zernike Institute for Advanced Materials (including the associate members).

Signatures

Applicant (the student applying for the PhD grant)

Date: 31/1/14

Name: M.E. Kamminga

Signature:

Daily PhD supervisor (only needed if applicable, in case of supervision by an assistant professor or UD/UHD without ius promovendi)

Date:

Name:

Signature:

1st Promotor (staff member with ius promovendi)

Date:

Name:

Signature:

31/1/14

T PALSTRA